The 2010 IEEE/RSJ International Conference on
Intelligent Robots and Systems
October 18-22, 2010, Taipei, Taiwan

Tetrabot: Resonance Based Locomotion for Harsh Enviroments

Jonas Neubert, Student Member IEEE, Jon Stockton, Ben Blechman, Hod Lipson, Member IEEE

***Abstract*— We describe a robotic architecture that combines the benefits of existing enclosed robots with passive dynamics. This combination results in a mobile robot with no moving parts exposed to the environment, making it ideal for tasks where wheeled or legged robots fail. Instead of suppressing resonance, the new robot morphology relies on the dynamics of resonance for locomotion. Actuators mounted on a central sphere excite a natural mode of vibration by pulling on strings through which the sphere is mounted to a tetrahedral frame. A simple open loop controller is sufficient to cause directed motion by hopping and sliding in a prototype. Rolling as a further gait is investigated theoretically. Fully enclosed resonant dynamic robots could lead to a new type of robot locomotion powered from a vibration source only. This is useful in the microscale where traditional actuators are not available, and at the macroscale where the robot's high ruggedness is favorable.**

I. INTRODUCTION

THE vast majority of mobile robots to date achieve locomotion through external actuators on the outer side of the robot body. Most frequently these are wheels or legs, each being actively controlled so that every movement of the actuator corresponds to a desired change in robot position. Wheels are often favored because two actuators are sufficient to provide two degrees of freedom for a planar robot and the transformation between actuator motion and robot motion is easy. Legged robots are commonly seen as a biomimetic alternative to wheeled robots and are usually capable of navigating more complex terrain. Both wheeled and legged robots have the disadvantage that the mechanically complex actuated joints are closest to the ground and therefore prone to damage by external influences like sand, moisture, temperature or radiation. The conventional solution to this problem is to design the actuators for harsh environments, for example by including seals and guards.

In this paper, we approach the task of robot locomotion in harsh environments from a dual perspective. First, we present exploratory work towards a new robot morphology that keeps all actuators enclosed in a rigid protective hull. Second, we propose a move away from the concept of employing simple transformations between actuator space and geometric space towards a locomotion system that uses continuous oscillations to achieve multiple modes of locomotion with a small number of actuators.

Manuscript received March 10, 2010. This work was supported in part by the U.S. National Science Foundations Office of Emerging Frontiers in Research and Innovation, grant #0735953, and Cornell University funds for undergraduate research. J. Neubert would like to thank the Institution of Mechanical Engineers and the Old Centralians Trust of the City and Guilds College Association for their financial support.

J. Neubert and H. Lipson are with the Computational Synthesis Laboratory, Cornell University, Ithaca, NY, 14853 USA (e-mail: jn283@cornell.edu, hod.lipson@cornell.edu, phone: 607-254-8940).

B. Blechman and J. Stockton are graduates of Cornell University, Ithaca, NY, 14853 USA, both with MEng and BS degrees in Mechanical Engineering (e-mail: jfs32@cornell.edu, bjb47@cornell.edu).

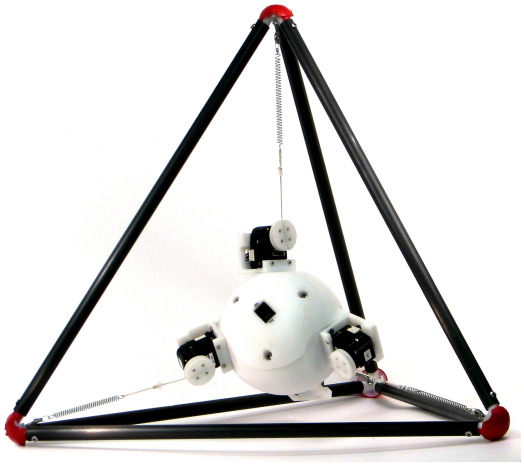

Fig. 1. Tetrabot. The robot has a tetrahedral frame that can be fully enclosed. A central sphere containing all actuators is mounted to the frame through four springs. After closing the faces with any rigid or flexible enclosure, the robot is ready to operate in mud, dust and even water without any modifications to the actuators.

Mobile robots that either enclose or could enclose all actuators and moving parts have been presented in the past. Several types of spherical rolling robots have been demonstrated [1]. Their methods of generating robot movement range form internal wheels [2] and gyroscopic motion [3] to changing the center of gravity [4]. Besides rolling robots, some other modes of locomotion have been presented for fully enclosed robots: Tensegrity structures have been suggested for locomotion [5], an enclosed hopping robot for planetary exploration was presented in [6], and a concept for spherical robots that hop and roll was presented in [7].

The robot presented in this paper – Tetrabot – is similar to many of the aforementioned enclosed robots by having a rigid frame (optionally covered by a hull) inside which all actuators are carried. Instead of employing methods of locomotion that are targeted towards one specific gait such as hopping or rolling, our robot is based on the principles of passive dynamics. In living organisms, both for legged locomotion with any number of legs and non-legged locomotion (e.g. crawling and sliding) the generation of movement is based on oscillation. Imitating this way of moving has in the past led to the development of passive dynamics, which has been scope of much research over recent years, mainly focusing on bipedal walkers, for example in [8], [9], and [10].

Passive dynamics is based on the storage of potential

energy within a structure, for example in the form of momentum of swinging limbs. Like locomoting systems in nature, passive dynamic robots are inherently stable and actuators are usually not linked to a particular joint but serve to keep the energy level within the structure constant. This is, for example, demonstrated by passive dynamic walkers which advance down a slope in a walking gait without any control or actuators [11]. We propose to extend this concept towards machines that continuously and actively excite their own natural frequency with the goal of locomotion. This is in stark contrast to common engineering practice that strives to avoid or suppress resonance in the design of machines.

Basic examples of locomotion caused by oscillating excitation can be observed in everyday technology. For instance, the vibration alert of a mobile phone causing the phone to traverse over a table can be considered a primitive example of resonant dynamic locomotion. The same principles are frequently used for hobbyist robotics projects referred to as BEAM robots [12], for example the popular Bristlebot [13]. These effects can be amplified using material properties such as directional friction. Tetrabot extends this technique towards large robots and for directed locomotion. This paper begins by introducing dynamics and control of Tetrabot, then elaborates on the optimization technique and simulation used to find suitable controllers, and subsequently presents results from both simulation and mechanical prototype.

II. METHODS

A. General Mechanism Design

To investigate the concept of locomotion through resonant dynamics we constructed a robot consisting of a tetrahedral rigid frame and a central mass suspended from the frame. Note that this general concept could be realized at many scales ranging from nano-scale to macro-scale. The frame comprises six edges which are connected by four spheres located at the tetrahedrons vertices. When resting, three of these vertices touch the ground while the remaining one is at the topmost position of the frame.

The central mass of the robot is connected to the frame through four springs. Each spring is mounted with one end to one of the frame's vertices and with its other end to the central mass. Central to the robot design is that the location of the spring end point closest to the central mass can be varied. Tetrabot implements this concept by mounting each spring to a pulley which is turned by a rotary servo actuator mounted to the robots central mass as illustrated in Fig. 2 (b) and (f).

Ignoring rotation of the central sphere nine equations of motion can be derived:

$$m_f \ddot{u}_{i,f} + 4k(u_{i,f} - u_{i,s}) = 0 \tag{1}$$

$$m_s \ddot{u}_{i,s} + 4k(u_{i,s} - u_{i,f}) = 0 \tag{2}$$

$$J_{\theta i} \ddot{\theta}_i = 0 \tag{3}$$

where k is the spring constant, m a mass, u_i a Cartesian coordinate, θ_i an angular coordinate, subscript f denotes frame, subscript s the central mass and $J_{\theta i}$ the moment of inertia about θ_i. During the derivation of these expressions the simplifying assumptions were made that the spherical connectors at each edge and the enclosure wrapped around the robot are of negligible weight and the edges of the robot were modeled as point masses. The analysis is greatly simplified by the fact that moments of inertia are equal about any axis for both Platonic bodies (such as the tetrahedron) and spheres.

Equations 1 through 3 are of only limited use because they do not include any constraints and can therefore not yield information about locomotion relative to another object such as ground. One can, however, use them to determine the natural frequencies ω_n of Tetrabot (same notation as Equation 3):

$$\omega_n = \sqrt{(4k)/m_s}, \sqrt{(4k)/m_f}. \tag{4}$$

Further development of an analytical model of Tetrabot requires the addition of constraints for ground and friction. For the general case this would result in a hybrid model with different states for various phases of the motion. A simplified model for the case of rolling is readily developed, we will present this in Section III-D.

B. Robot Actuation and Control

A range of control algorithms for control of the four rotary actuators contained in the robot were considered. While closed loop control is a possibility, implementing the required sensing capabilities with sufficient resolution and accuracy would be contrary to the simplistic concept of resonant locomotion. We therefore focus on a simple open loop controller based on the summation of harmonic (sinusoidal) oscillations. The controller output is an angular set point for the servo actuator.

Each motor's set point is calculated as the sum of n sine waves with fixed frequencies, i.e.

$$x = \sum_{i=1}^{n} (A_i + B_i sin(C_i t + D_i)). \tag{5}$$

Because any signal can be represented as the sum of sine waves, with a high enough n, a wide range of signals can be generated. Given the number of motors m (four in the case of a tetrahedral frame) the space of controller parameters that requires searching to find useful controllers contains

$$L = 4 * m * n \tag{6}$$

combinations of the parameters A to D (offset, amplitude, frequency and phase shift of the respective sine wave).

C. Controller Optimization

A genetic algorithm was used to search the space of L possible controllers. Genetic algorithms evaluate and rank an initial randomly generated population of individuals according to a fitness criterion. By means of recombination and mutation of the individuals of this first generation, a new generation is created which is again evaluated and forms

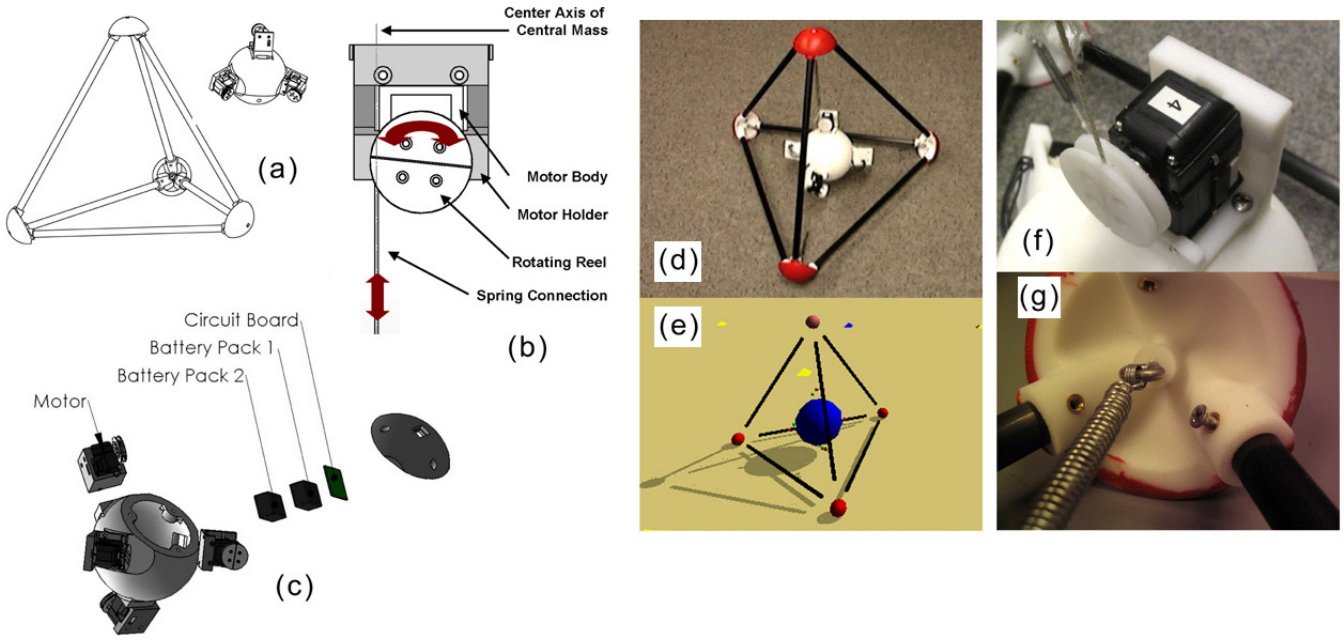

Fig. 2. Robot Layout. (a) Schematic of tetrahedral frame and central sphere. (b) A rotary actuator with pulley is used to shorten the length of the spring. (c) Exploded view of the central sphere assembly. (d) The robot prottoype. (e) Visualization of physics simulation collision bodies. (f) Photo of actuator mounted to central sphere. (g) The vertices were produced using fused deposition modeling and subsequently coated with (red) rubber to increase friction.

the basis for yet another generation. Repeating this process mimics natural evolution.

Each individual needs to be represented as a chromosome consisting of genes which in some defined way map to the controller properties. For the purpose of evolving our controllers, a chromosome is represented by an array of floating point numbers of the length L as defined in Equation (6). Each gene stands for one of the parameters of the controller with the mapping being arbitrary but constant.

To evaluate the fitness of a chromosome the resulting controller was implemented to control the robot's behavior in a physics simulation. The simulation duration was kept constant at 7.5 seconds and each individual starts from rest. The distance traveled during this time was used as the fitness metric for each individual.

A standard genetic algorithm with an elitism based selection criterion was used [14] and implemented using a modified version of the Fast Genetic Algorithm C++ library [15]. For each chromosome within a generation of size 100 the fitness was found and used to rank the chromosomes. The best 50 chromosomes were chosen in pairs at random to generate replacements for the 50 worst. Mating was between disparate parents only and generated two offspring by two-point crossover and random mutation at a rate of 5%. The evolutionary search was automatically terminated when the population had converged with the convergence criterion being that for all genes 95% or more of the chromosomes of one generation share an identical value.

Genetic algorithms are only superior to other optimization methods if the fitness landscape has multiple maxima. To establish if this is the case, both a genetic algorithm and a hillclimbing algorithm were run three times each with randomly generated initial populations for controllers with 2, 4 and 8 superimposed sine waves. For all cases did the genetic algorithm find better solutions before converging than the hillclimber which settled at a local maximum of the fitness landscape. This indicates that the choice of a genetic algorithm for optimization of the controller is suitable in this case. The difference in performance between hillclimber and genetic algorithm was higher for higher numbers of parameters (i.e. for controllers with more sumperimposed sine waves).

TABLE I
CONTACT JOINT SIMULATION PARAMETERS

Contact Mode	dContactApprox1 || dContactSoftCFM
Coulomb friction coefficient	5.0
Coulomb friction coefficient (2nd direction)	5.0
Constraint Mixing Force Parameter	0.1

D. Physics Simulation

The need for a virtual model of the robot arises when evolutionary optimization of a robot controller with genetic algorithms is intended. A genetic algorithm requires

$$m = g * s_{population} \tag{7}$$

trials where g is the number of generations before convergence and $s_{population}$ the number of chromosomes whose fitness needs to be evaluated for each generation. When

TABLE II
PROTOTYPE DESIGN PARAMETERS

Mass of frame	776g
Mass of central sphere	1392g
Tetrahedron side length	480mm
Radius of center sphere	70mm
Spring constant	360N/m

hundreds of generations with a population size of 100 are required, as it is the case for our parameter search, it is unfeasible to conduct an experiment with such a large number of trials in reality.

Physics simulation engines model the rigid body dynamics by taking into account forces and impacts to compute properties of objects, for example impulse and acceleration, for successive time steps. We chose the open source software ODE [16] which additionally provides collision detection and comes with a rudimentary visualization library. Due to the computational complexity of rigid body simulation and the large number of simulations run by the genetic algorithm, modeling the detailed geometry of a real robot is infeasible. For our purposes the use of two basic geometric bodies, spheres and cylinders, proved sufficient to model the geometry and mass properties of the robot.

The extension springs connecting robot frame with the central mass are modeled as a separate C++ class applying appropriate forces at the mounting points of the spring. Particular care had to be taken regarding the geometric precision of the spring model because even minor variations result in significant changes to the dynamic behavior of the robot. Instead of implementing the rotary actuators in much detail, only the mounting point of the spring on a disk connected to the motors output shaft which results from motor rotation was implemented in simulation. To realistically simulate DC motors the actuators' speed of rotation was bounded at 1.130 rad/s and it's acceleration was smoothed.

Physics simulation engines do not solve the differential equations governing object behavior but instead rely on numerical approximations. When investigating locomotive behavior of a robot in ODE this becomes most apparent in the surface interaction of the bodies. Several approximation models are available in ODE for each of which a set of parameters can be defined. For our robot we found the most appropriate parameters through trial and error in comparison between the behavior of the robot vertices in simulation and those of the prototype. This resulted in the use of a contact model combining a "friction pyramid" model to simulate friction with a constraint mixing force to give the contact softness (see [17] pp. 33-36) with the parameters given in Table I. A visualization of the complete model generated is shown in Fig. 2 (e).

E. Mechanical Prototype Design

Based on the knowledge gained from the physics simulation of the robot we further showed the feasibility of the concept of a fully enclosed robot using resonant dynamics by building a tetrahedral prototype (see Fig. 2 (d)). As in the simulated robot, each of the four vertices of the tubular frame is connected to the robot's central mass via an extension spring. All passive parts of the robot apart from the carbon fiber tubes in the frame were manufactured using ABS plastic by fused deposition modeling (3D printing). The detail design of parameters such as masses and lengths was an iterative process aided by the qualitative findings from the robot simulation described above. The final design parameters of the prototype are given in Table II.

The actuators used to change the location of the mounting point of the extension spring are Dynamixel DX-117 type motor packs distributed by Robotis Inc. Besides a DC motor the compact actuator package includes gearing and a motor controller implementing PID control. Communication with the package is by a serial communication interface. A RS-485 cable connects every actuator to a central controller board of type CM5Plus which is also from Robotis Inc. The board features an Atmel Atmega128 controller which was programmed in C.

The central mass is a hollow shell assembled from two parts making up a spherical part and four robot mounting clamps. The wall thickness of the inner shell was arbitrarily chosen 10mm with the inside space being sufficiently big to house the CM5Plus controller board as well as two 15V battery packs with 2200mAh capacity each and additional ballast weights. These components were arranged in a way giving an approximately balanced mass distribution.

The spheres located at the vertices in the simulation model were replaced by shelled spherical sections. Increased friction was provided by a rubber surface coating.

III. RESULTS

A. General Observations from Simulation

In simulation, three types of motion have been achieved: Hopping of the robot, sliding of the vertices, and a combination of both. More complex frame shapes were investigated briefly and some showed a tendency to roll.

The fittest controller evolved actuates the motors close to a natural frequency of the structure with shifted phases. Resonance was not favored in the fitness function of the genetic algorithm and the fact that it was present in the fittest candidate can be seen as a confirmation of resonance as a means of generating locomotion for the given mechanism. The maximum distance covered during the simulation time of 7.5s was 56 cm equaling a speed of 4.48m/min. Note that the path taken by the robot is not taken into consideration.

B. General results and gaits observed from prototype

To test whether the results obtained in simulation translate to reality we implemented the best performing simulated controllers with two superimposed sine waves in the robot prototype described above. As a minor modification the already very similar frequencies of the different sine waves were rounded to make them equal. This is to continuously see one "gait" of the robot instead of a continuously varying pattern. It is unrealistic to expect our optimization to

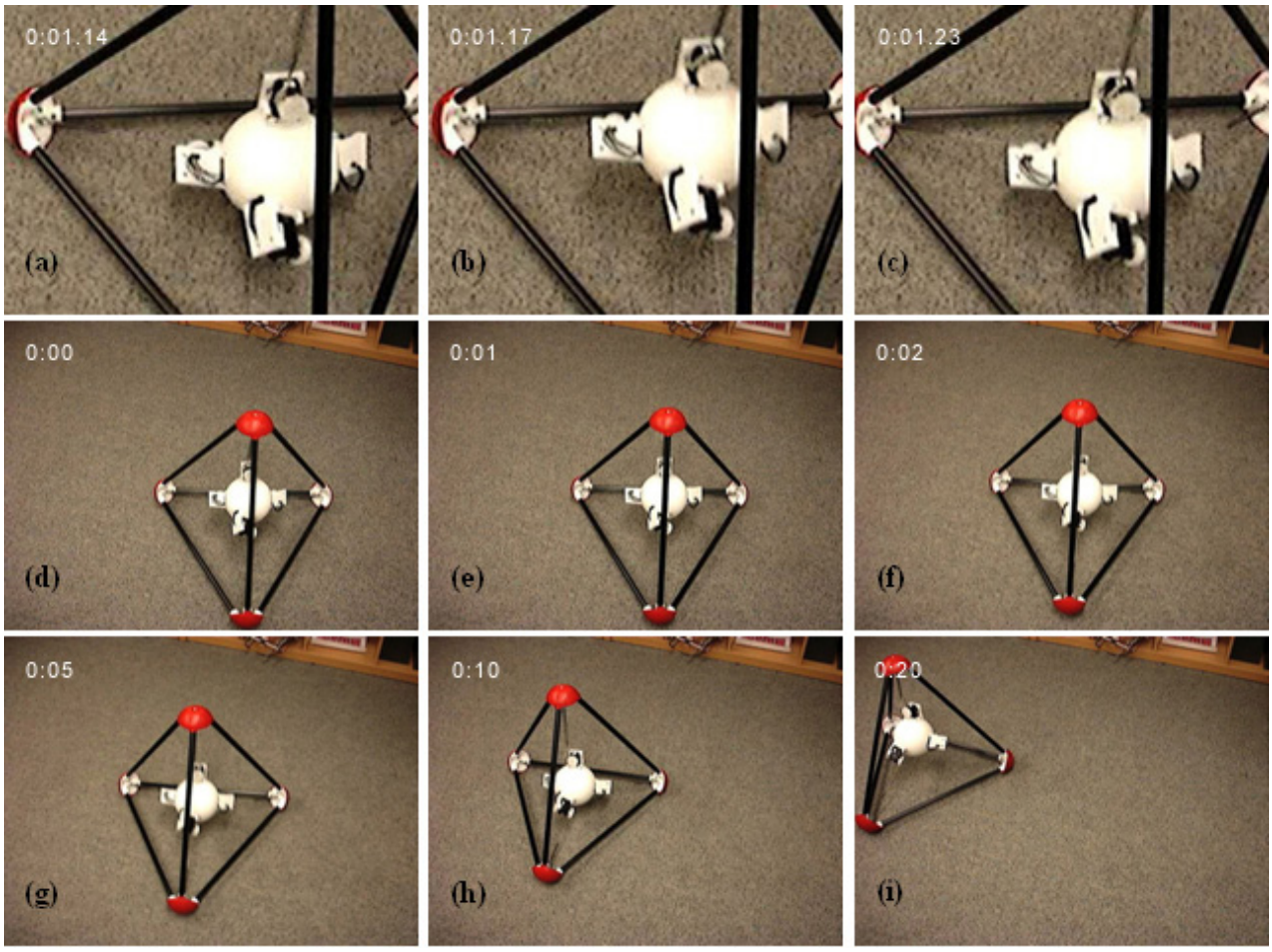

Fig. 3. Robot Locomotion. One of the observed gaits showed the robot lifting all vertices off the ground at every other period of oscillation. This jump is shown in sequence (a) to (c). The point at which no vertex is in contact with ground is between frames (b) and (c). The speed achieved with this gait was 2.3 m/min, the frames show the robot after (d) 0s, (e) 1s, (f) 2s, (g) 5s, (h) 10s and (i) 20s.

account for this because the simulated interval spans only 7.5 seconds.

The gait observed for the prototype was hopping such that the entire robot lifts off the ground repeatedly intermitted by short periods of resting and some sliding. The observed hopping involves lifting off the ground for up to 5cm. This gait yields movement on a variety of surfaces including soft carpet and smooth tiled floor. A maximum speed of 2.3 m/min was measured; an image sequence of the movement is shown in Fig. 3 and a video is available as supplementary material. The observed movement was always in one repeatable direction relative to the robot's coordinate frame during tests in various locations and settings. It is easy to see that by permutating the motor assignments, movement in three directions spaced by 120° can be generated from one controller. By combining these directions, overall movement in any direction can be generated.

The difference to the speeds observed in simulation is due to the fact that it was not possible to simulate the surface interaction and dynamic behavior accurately enough to quantitatively predict the behavior of the prototype from simulation. Qualitatively the results from simulation and prototype experiments do correlate. This is shown by the fact that the controller optimized in simulation and tested on the prototype described a path slightly curved towards the right while other controllers developed by trial and error with the prototype described a path curved to the left both in reality and in simulation.

TABLE III
POWER CONSUMPTION OF PROTOTYPE

Gait No	No of superimposed sine waves	Average Power consumption over 20 sec period
1	10	3.06
2	1	2.86
3	25	3.11
not moving	0	0.77

C. Energy Consumption

To benchmark resonant dynamic locomotion against other forms of locomotion, the energy consumption of the prototype was investigated. Three different controllers were run on the robot, each with a different number of superimposed sine waves. A further measurement was carried out with no

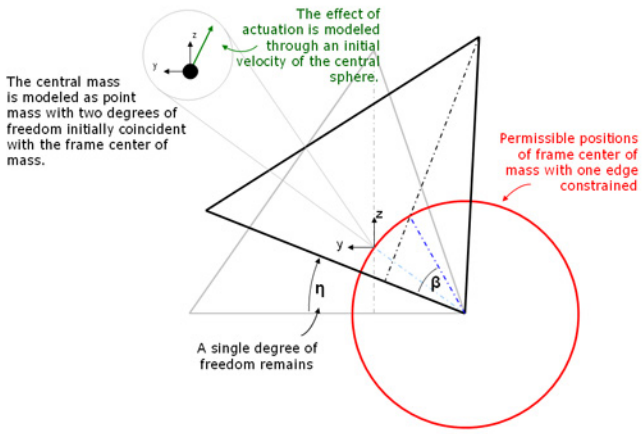

Fig. 4. Schematic of simplified model of Tetrabot tipping over its edge. The grey triangular shape is a crossection of Tetrabot at rest, the black triangle at an arbitrary point during rolling. The bottom left corner is constrained.

motor movement to establish which proportion of the power is due to continuous power consumption by the electronic components. The results of these experiments are shown in Table III.

The average power consumption was calculated from the measured current and set voltage over a period of 20 seconds for each controller (always including the startup phase during which increased energy input into the system is required because the center mass needs to be accelerated from rest). Current consumption was sampled at a rate of 1 kHz. The average power consumption was 3.00W averaged for all measurements, 0.77W of which are consumed by the robot at rest. Given a capacity of 2200mAh for both batteries packs, this equates to a theoretical duration of operation of 22 hours.

D. Analysis of rolling motion

Hopping and sliding were observed in the robot's gait, but rolling was not. Making the simplifying assumption that Tetrabot rolls over one of its edges which is assumed fixed, leaves one rotational degree of freedom η for the frame and two planar degrees of freedom for the central sphere. The constraint equations for this simplified case are

$$x_f = x_s = 0 \tag{8}$$

$$y_f = r_i scos(\beta) - r_i scos(\beta + \eta) \tag{9}$$

$$z_f = -r_i ssin(\beta) - r_i ssin(\beta + \eta) \tag{10}$$

$$\theta_1 = \eta, \theta_2 = \theta_3 = 0 \tag{11}$$

where the same notation as in Section II-A is used with the exception of the Cartesian coordinates being renamed to x, y, and z. β is defined in Fig. 4. Obtaining the equations of motion using Lagrange multipliers and numerical integration in Matlab yields that the frame can tip if the central sphere reaches speeds of 1.4m/s. This is feasable given our current prototype setup, but the friction to enforce the assumed constraint is not available. The robot slides before it starts rolling, an issue potentially overcome by other frame geometries as investigated by [18].

IV. CONCLUSION

We demonstrated a mechanism design that can be fully enclosed by a protective skin without exposing any actuators. Such a robot is in theory resilient against most environmental conditions such as particles and moisture. Furthermore, we have demonstrated a robot able to move in a directed way using a harmonic oscillator as only actuator type. This proves that resonant dynamic locomotion is possible. Paired with the observation that rolling gaits might be achievable with other frame shapes, this makes resonant dynamic locomotion a candidate mode of propulsion for environments where traditional methods fail. Additionally, the concept of an enclosed robot powered by oscillation could be beneficial at small scales where rotary actuators are not available.

REFERENCES

[1] V. Crossley, "A Literature Review on the Design of Spherical Rolling Robots," Pittsburgh, PA, 2006.

[2] A. Halme, T. Schonberg, and W. Yan, "Motion control of a spherical mobile robot," in *International Workshop on Advanced Motion Control*, vol. 1. IEEE, 1996, pp. 259–264.

[3] S. Bhattacharya and S. Agrawal, "Design, experiments and motion planning of a spherical rolling robot," in *ICRA 2000*. San Francisco: IEEE, 2000, pp. 1207–1212.

[4] A. Javadi and P. Mojabi, "Introducing August: a novel strategy for an omnidirectional spherical rolling robot," in *ICRA*. Washington, DC: IEEE, 2002, pp. 3527–3533.

[5] J. Rieffel, F. Valero-Cuevas, and H. Lipson, "Morphological communication: exploiting coupled dynamics in a complex mechanical structure to achieve locomotion," *Journal of the Royal Society Interface*, vol. 45, no. 7, pp. 613–621, 2010.

[6] P. Fiorini, S. Hayati, M. Heverly, and J. Gensler, "A hopping robot for planetary exploration," in *Aerospace Conference*, vol. 2. Snowmass at Aspen: IEEE, 1999, pp. 153 – 158.

[7] S. Dubowsky, K. Iagnemma, S. Liberatore, D. M. Lambeth, J. S. Plante, and P. J. Boston, "A Concept Mission: Microbots for Large-Scale Planetary Surface and Subsurface Exploration," in *Intl. Forum for Space Technology and Applications*, M. S. El-Genk and M. J. Bragg, Eds., vol. 746, no. 1. Albuquerque, NM: AIP, Feb. 2005, pp. 1449–1458.

[8] T. McGeer, "Powered flight, child's play, silly wheels and walking machines," in *ICRA 1994*. Scottsdale, AZ: IEEE, 1994, pp. 1592 – 1597.

[9] S. Collins, A. Ruina, R. Tedrake, and M. Wisse, "Efficient bipedal robots based on passive-dynamic walkers." *Science*, vol. 307, no. 5712, pp. 1082–5, 2005.

[10] F. Iida, J. Rummel, and A. Seyfarth, "Bipedal Walking and Running with Compliant Legs," in *ICRA*. Rome: IEEE, 2007, pp. 3970–3975.

[11] M. Garcia, A. Chatterjee, A. Ruina, and M. Coleman, "The simplest walking model: stability, complexity, and scaling." *Journal of biomechanical engineering*, vol. 120, no. 2, pp. 281–8, 1998.

[12] D. Hrynkiw and M. W. Tilden, *JunkBots, Bugbots, and Bots on Wheels: Building Simple Robots With BEAM Technology*. McGraw-Hill, 2002.

[13] W. H. Oskay, "Bristlebot: A tiny directional vibrobot," 2007. [Online]. Available: http://www.evilmadscientist.com/article.php/bristlebot

[14] M. Mitchell, *An introduction to genetic algorithms*. MIT Press, 1998.

[15] A. Presta, "Fast Genetic Algorithm (FGA)," 2006. [Online]. Available: http://fga.sourceforge.net/

[16] R. Smith, "Open Dynamics Engine (ODE)," 2007. [Online]. Available: http://ode.org/

[17] ——, "Open Dynamics Engine v0.5 User Guide," 2006. [Online]. Available: http://ode.org/ode-latest-userguide.pdf

[18] P. Lingane, "Design of an Auto-Rolling Ployhedron," MEng Thesis, Cornell University, 2010.